Determination of the Composition of Delavirdine Mesylate Polymorph and Pseudopolymorph Mixtures Using ^{13}C CP/MAS NMR

Ping Gao[1,2]

Received January 5, 1996; accepted April 17, 1996

Purpose. The application of solid-state nuclear magnetic resonance for the quantitation of relative amounts of delavirdine mesylate (DLV-M) polymorph and/or pseudopolymorph in their binary mixtures is presented.

Methods. ^{13}C CP (cross-polarization)/MAS (magic angle spinning) NMR techniques were employed for quantitation.

Results. ^{13}C CP/MAS NMR spectra of three DLV-M solid forms (VIII, XI, and XII) revealed distinct differences in chemical shifts and peak splitting characteristics. Resonances of isopropyl methyl carbons of DLV-M were diagnostic of each form; resonance intensities were utilized to determine the composition of two series of DLV-M solid form mixtures (VIII and XI; XII and XI) over a dynamic concentration range (1–50%). The empirical detection limit of form VIII, or XII, in a dominant form XI environment was about 2–3% (w/w). Quantitations were obtained using appropriate analytical procedures, which took into account the differences of T_{CH} and $T_{1\rho H}$ between the two forms. Quantitative results obtained using either the peak area or peak height were examined, and, in general, were satisfactory.

Conclusions. The methodology and analytical procedure developed in this study are generally applicable to quantitative analysis using ^{13}C CP/MAS NMR for pharmaceutical solids, including bulk drug substances, and dosage forms. Reliable measurement of NMR relaxation times ($T_{1\rho H}$) and CP rate constants (T_{CH}) of individual forms is a critical component in this application.

KEY WORDS: polymorph; pseudopolymorph; solid-state nuclear magnetic resonance; ^{13}C CP/MAS NMR; relaxation times.

INTRODUCTION

Polymorphism is a major issue in the pharmaceutical industry, where health and safety legislation is becoming increasingly stringent, because different polymorphs usually show different drug release profiles *in vivo*. Delavirdine mesylate (DLV-M) (structure shown below) is a potent non-nucleoside reverse transcriptase inhibitor being developed for the treatment of Acquired Immune Deficiency Syndrome (1–2). DLV-M crystallizes in a variety of solid modifications (3). Forms VIII, XI, and XII are all crystal forms of this chemical entity. Both forms VIII and XI are nonhygroscopic anhydrates, while form XII is a pseudopolymorph which may contain non-stoichiometric amounts of solvent or water (3). Form XI is the preferred solid form for formulation because of its superior thermodynamic stability and acceptable bioavailability.

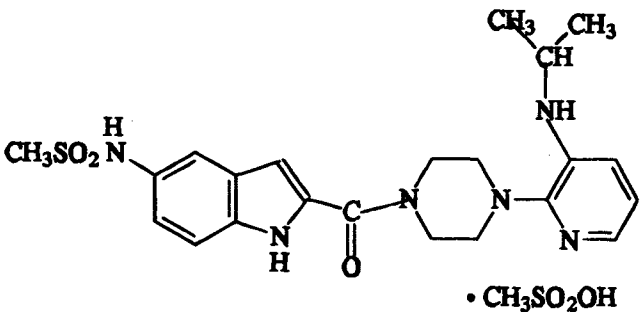

Scheme I.

Identification and characterization of DLV-M polymorphs and pseudopolymorphs were a critical component of the formulation development for delavirdine mesylate. Inappropriate polymorphs or pseudopolymorphs of DLV-M need to be detected, quantified, and controlled during manufacturing. Solid state ^{13}C NMR spectroscopy is one of the major analytical techniques in the characterization of pharmaceutical solids (4–9). ^{13}C spectra acquired using a combination of cross-polarization (CP) for sensitivity enhancement, with magic-angle spinning (MAS) and high power proton decoupling for resolution enhancement, have been extensively used to identify and characterize pharmaceutical polymorphs in bulk drug substances and dosage forms (4–9). There are a number of significant advantages which make ^{13}C CP/MAS NMR particularly well suited for investigating polymorphism in pharmaceuticals. First, it has been demonstrated that the chemical shift of polymorphs is sensitive to molecular conformation and chemical environment in the crystal lattice (4–9). Second, the investigation of polymorphism can be performed at either the drug substance or the dosage form stage (4,6,8,9). This ability allows one to investigate polymorph phase interconversion under various processing techniques (e.g., dry blending, lyophilization, tableting, and fluidized-bed granulation). Third, the signal intensity of a particular resonance in a NMR experiment can be directly related to the number of nuclei producing it under *appropriate* experimental condition and analytical procedures without calibration efforts (10). Despite a number of publications describing the use of solid-state NMR for polymorphic characterization, the majority have dealt with *qualitative* studies only briefly alluding the possibility of quantitative analyses (4–9). There have been few *quantitative* studies of pharmaceutical polymorphs reported (11).

This work focuses on the detection and quantitation of relative amounts of a minor DLV-M polymorphic form (VIII) or pseudopolymorphic form (XII) in a major form (XI) environment using ^{13}C CP/MAS NMR. These binary mixtures of DLV-M solid forms were prepared and examined by ^{13}C CP/MAS NMR techniques to study quantitative reliability of the technique. It is our intent to develop appropriate solid-state NMR methods to investigate pharmaceutical materials of broad interest (e.g., polymorphs, pseudopolymorphs, solvates, excipients, dosage forms, etc.). With inherently good signal dispersion and detectability, as demonstrated in this study, ^{13}C CP/MAS NMR techniques are extremely valuable for both qualitative and quantitative characterization of pharmaceutical solids.

[1] Analytical Research and Specifications Development, Pharmacia & Upjohn, Incorporated, Kalamazoo, Michigan 49001.

[2] To whom correspondence should be addressed.

0724-8741/96/0700-1095$09.50/0

MATERIALS AND METHODS

Forms VIII, XI, and XII of DLV-M were isolated in the research laboratories of Pharmacia & Upjohn, Inc. Two series of DLV-M binary mixtures were prepared and examined: a series of mixtures of forms VIII and XI and a series of mixtures of forms XII and XI. These mixtures were prepared by weighing and blending the parent lots of a pure form. The mass fraction of form VIII, or XII, in the mixtures with form XI is denoted by either w_{VIII}^{mass}, or w_{XII}^{mass} (%, w/w). About 200 mg of each sample was packed into a zirconium dioxide rotor (7 mm diameter) for CP/MAS NMR measurement.

A Bruker MSL-200 NMR spectrometer with an Oxford wide-bore (89 mm) magnet was used. The static field of the superconducting magnet was 4.7T, the spectrometer operated at 50.3 MHz for ^{13}C and 200.055 MHz for ^{1}H. A doubly tuned, single-coil CP/MAS double gas bearing type probe (Bruker) was employed. The magic angle was adjusted using a KBr sample (12), which afforded a spinning angle of 54.7° ± 0.3°. Hartmann-Hahn matching was optimized using admantane and kept for subsequent DLV-M experiments. ^{1}H decoupling was applied with an on-resonance ^{1}H RF field of 72 kHz. The samples were usually spun at a spinning speed of 3.5 kHz or 4.5 kHz ± 2Hz, which was sufficient to suppress the spinning side bands due to methyl groups (used for quantitation).

Proton spin-lattice relaxation times in the laboratory frame (T_{1H}), proton spin-lattice relaxation times in the rotating frame ($T_{1\rho H}$), and the heteronuclear cross-polarization transfer rate constants (T_{CH}) were measured through CP/MAS related pulse sequences via the detection of carbon signals (13). A ^{1}H flipback pulse sequence was employed (13) and the repetition time between successive sampling pulses was 5 sec. The acquisition parameters were: spectral width, 20 kHz; contact time, 2 ms; and 3.5 μs 90° ^{1}H pulse. Each spectrum was obtained with 2K data points, zero filling to 8K with 20 Hz line broadening prior to Fourier transformation. ^{13}C chemical shifts were calibrated indirectly to the higher field adamantane peak (29.5 ppm relative to tetramethylsilane). All curve fitting and plotting were performed with SigmaPlot 5.1.

RESULTS AND DISCUSSION

^{13}C CP/MAS NMR of DLV-M Solid Forms

The ^{13}C CP/MAS NMR spectra of DLV-M forms XI, VIII and XII, are shown in Figures 1A–1C, respectively. Notable differences are observed among the spectra. Form XII exhibits more resonances than forms VIII and XI, and the resonances of form XII are also significantly broader. In particular, the form XII spectrum (Figure 1C) exhibits a singlet at 19.1 ppm, and a doublet at 21.2 and 22.2 ppm in the upfield region (15–30 ppm). In contrast, an unique resonance is observed at 17.3 ppm for form VIII (Figure 1B) while a distinct 20.2 ppm resonance is only observed for form XI (Figure 1A). Both forms VIII and XI show carbon resonances at 23.9 ppm. All these resonances were assigned to the isopropyl methyls through the application of interrupted decoupling. The variation of the chemical shift of the isopropyl methyls among the three forms results from the differences of molecular conformation and packing; a detailed analysis of ^{13}C CP/MAS NMR features of these forms will be given in a separate report (14).

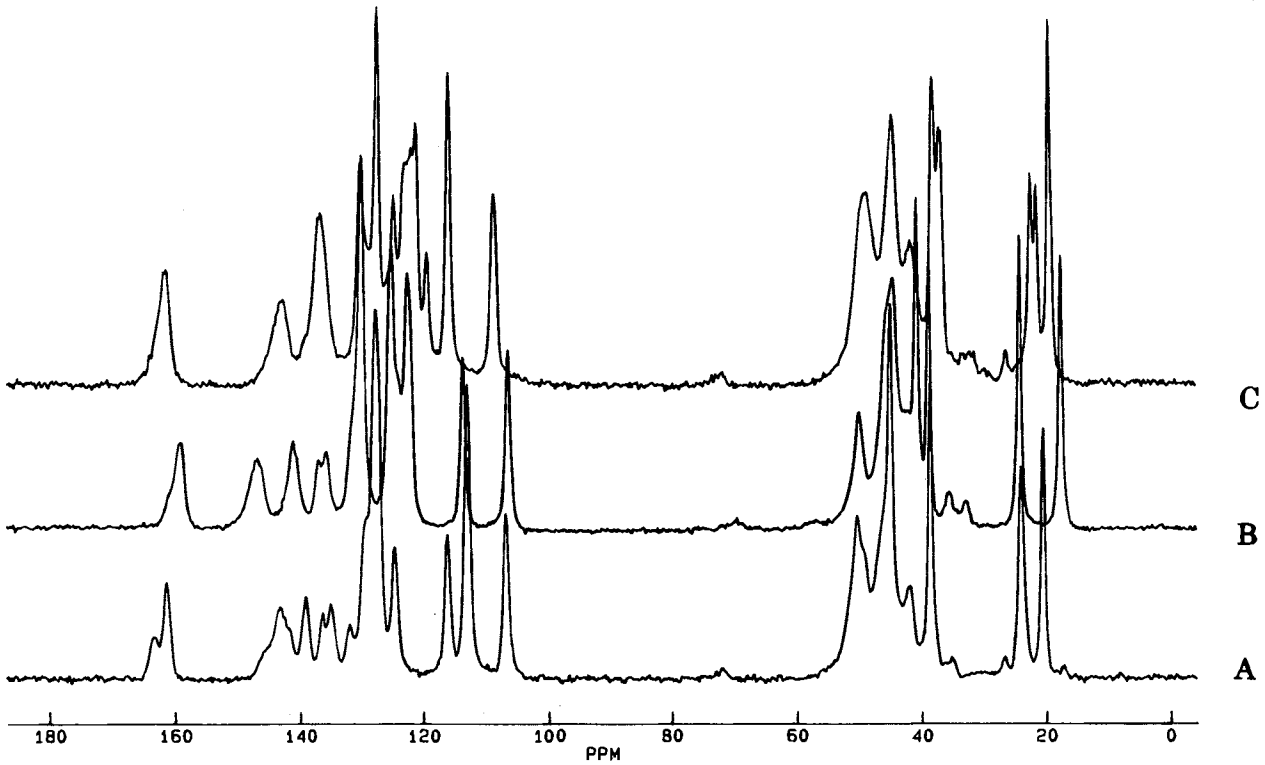

Fig. 1. ^{13}C CP/MAS NMR spectra of forms (A) XI, (B) VIII, and (C) XII. Spectra were obtained using contact time = 2 ms; spinning rate = 4.5 kHz; and scan number = 640.

The NMR spectra indicate that several resonances can be used to differentiate DLV-M solid forms and, therefore, to identify and quantify the minor form in the presence of a major form. As discussed above, the methyl resonances at 17.3 and 19.1 ppm are diagnostic of forms VIII and XII, respectively, whereas the 20.2 ppm resonance is unique to form XI. Utilizing these characteristic ^{13}C resonances, determination of the composition of DLV-M polymorph and/or pseudopolymorph mixtures using solid-state NMR is feasible.

NMR Relaxation Behavior

Several characteristic parameters of the system must be explicitly determined in order to obtain quantitatively reliable ^{13}C CP/MAS NMR spectra. Proton spin-lattice relaxation times in the laboratory frame, T_{1H}, were a determining factor governing the repetition rate of CP/MAS NMR experiments performed. Substantially different T_{1H} values (average over several ^{13}C resonances) are observed among DLV-M solid forms: 1.34 ± 0.03 s for form XI; 1.87 ± 0.04 s for form VIII; and 1.03 ± 0.08 s for form XII. In principle, a repetition time of five × T_{1H} is needed. Further examination of spectral intensities of individual DLV-M forms using different repetition times (5 to 20 s) by employing a flipback pulse showed insignificant variations (~5% with scans ≥600). Therefore, a repetition time of 5 s was uniformly employed in this study, greatly reducing data acquisition times.

Additional critical parameters were the heteronuclear cross-polarization rate constant, T_{CH}, and the proton spin-relaxation time in the rotating frame, $T_{1\rho H}$. T_{CH} is important for setting the optimal contact time ($\tau \approx 10\ T_{CH}$) of the CP/MAS NMR experiment. Further, both T_{CH} and $T_{1\rho H}$ have a significant influence on quantitation (*vide infra*). T_{CH} and $T_{1\rho H}$ were determined via the carbon resonance detection through the spin-lock experiment as a function of the contact time in the CP/MAS NMR experiment. Peak intensity was then fitted to theoretical models describing the crosspolarization kinetics. A commonly accepted model has been given by Mehring (15–17) and is shown in Eq. 1:

$$I(\tau) = \frac{M^0\left(\frac{\gamma_H}{\gamma_C}\right)\left[\exp\left(-\frac{\tau}{T_{1\rho H}}\right) - \exp\left(-\frac{\tau}{T_{CH}}\right)\right]}{1 - \frac{T_{CH}}{T_{1\rho H}}} \quad (1)$$

where $I(\tau)$ is the peak intensity for each ^{13}C resonance at variable contact time (τ), γ is the gyromagnetic ratio, and M^0 is the thermal equilibrium value of the ^{13}C magnetization. $T_{1\rho H}$ and T_{CH} are usually simultaneously obtained through a three-parameter (M^0, $T_{1\rho H}$, T_{CH}) non-linear least squares fit to Eq. 1 (15–17).

The ^{13}C CP/MAS NMR spectra of each DLV-M form were recorded as a function of varied contact time. The resonance intensities of the methyl groups of these forms are plotted against the contact time (τ) in Figure 2. For each form, only two ^{13}C resonance intensity-contact time curves are selectively presented for illustration. As shown in Figure 2, the increase in ^{13}C intensities for shorter contact times ($\tau < 2$ ms) is due to T_{CH} effects, whereas the decrease in intensities for longer contact times is due to $T_{1\rho H}$ effects. The interrelation between these two competing mechanisms ultimately governs the kinetics of magnetization built-up in the CP experiment.

An unrestricted fit of the experimental data to Eq.1 was conducted to extract $T_{1\rho H}$ and T_{CH} (15–16). The $T_{1\rho H}$ values of

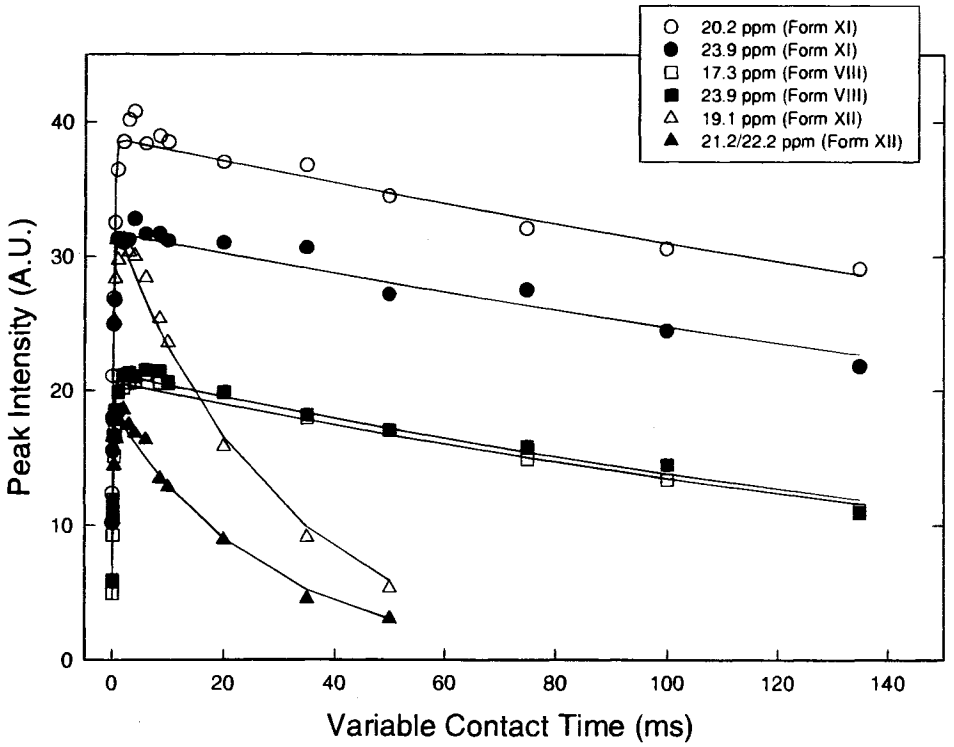

Fig. 2. Evolution of ^{13}C peak intensities of forms XI (○ 20.2/● 23.9 ppm), VIII (□ 17.3/■ 23.9 ppm) and XII (△ 19.1/▲ 22.2 ppm) as a function of the contact time. The solid curves are the best fit to Eq. 1.

the isopropyl methyls are: $T_{1\rho H}$(XI) = 447 ± 80 ms; $T_{1\rho H}$(VIII) = 234 ± 25 ms; and $T_{1\rho H}$(XII) = 27.5 ± 2.8 ms. As an uniform T_{1H} is observed in each form, essentially a single $T_{1\rho H}$ (with a standard deviation of 10%) is also observed using other ^{13}C resonances for individual forms XI, VIII, and XII. This is expected since protons exhibit fast spin diffusion in the solid state, and the proton relaxation reservoirs reequilibrate with the same time constant, resulting in a common $T_{1\rho H}$ for each form (15–16). The T_{CH} values of the isopropyl methyls are: T_{CH}(XI) = 0.20 ± 0.02 ms; T_{CH}(VIII) = 0.20 ± 0.02 ms; T_{CH}(XII) = 0.16 ± 0.02 ms. These constants are very similar, as expected (15). In contrast, the $T_{1\rho H}$ of form XII is significantly shorter than those of forms VIII and XI, whereas a small difference is observed between $T_{1\rho H}$ values measured for forms VIII and XI.

Measurements of T_{1H}, $T_{1\rho H}$, and T_{CH} of individual DLV-M forms in the mixtures were conducted in similar fashion utilizing their characteristic resonances. These measurements explored whether the characteristic cross-polarization and relaxation kinetics of each form were altered by mixing. Such measurements revealed that the T_{1H}, T_{CH}, and $T_{1\rho H}$ of forms VIII, XII, and XI in their 50% mixtures, respectively, remain virtually *unchanged.* This result suggests that the crystalline domain integrity of each form was properly maintained in the mixtures and not affected by blending and mixing. Nuclei within different domains, which act as isolated spin reservoirs, maintain their own characteristic spin kinetics. This is an important observation which supports the quantitation procedure discussed below.

Quantitation Using ^{13}C Intensity

Since ^{13}C resonance intensities of CP/MAS NMR spectra are governed by CP kinetics and proton relaxation processes as discussed above, reliable quantitation can only be achieved by taking into account the difference of CP and relaxation parameters of the resonances of interest (17–19). For a binary system, quantitation results can be expressed as a ratio between two components. Ratioing Eq.1 between polymorphs A and B, we obtain Eq. 2:

$$\frac{M^0_A}{M^0_B} = \frac{\left(1 - \frac{T^A_{CH}}{T^A_{1\rho H}}\right)\left[\exp\left(-\frac{\tau}{T^B_{1\rho H}}\right) - \exp\left(-\frac{\tau}{T^B_{CH}}\right)\right]}{\left(1 - \frac{T^B_{CH}}{T^B_{1\rho H}}\right)\left[\exp\left(-\frac{\tau}{T^A_{1\rho H}}\right) - \exp\left(-\frac{\tau}{T^A_{CH}}\right)\right]} \frac{I_A(\tau)}{I_B(\tau)}$$

$$= F_{A/B}\frac{I_A(\tau)}{I_B(\tau)} \qquad (2)$$

$$F_{A/B} = \frac{\left(1 - \frac{T^A_{CH}}{T^A_{1\rho H}}\right)\left[\exp\left(-\frac{\tau}{T^B_{1\rho H}}\right) - \exp\left(-\frac{\tau}{T^B_{CH}}\right)\right]}{\left(1 - \frac{T^B_{CH}}{T^B_{1\rho H}}\right)\left[\exp\left(-\frac{\tau}{T^A_{1\rho H}}\right) - \exp\left(-\frac{\tau}{T^A_{CH}}\right)\right]} \qquad (3)$$

where τ, $I(\tau)$, and M^0 are the same as defined previously in Eq. 1; the subscripts, A or B, refer to the two polymorphs A or B, respectively; and the term $F_{A/B}$ is defined in Eq. 3. Note that M^0 represents the *absolute number* of carbon atoms of each form. Therefore, Eq. 2 accounts for the ^{13}C intensity difference of two solid forms in a mixture as a result of their differences in T_{CH} and $T_{1\rho H}$ and correlates the quantitative information, M^0_A/M^0_B with the measurable resonance intensity ratio, I_A/I_B. Knowing T_{CH}, and $T_{1\rho H}$ of each form and the contact time (τ), the term $F_{A/B}$ is readily computed for quantitation purposes.

Quantitation of Form VIII and XI Mixtures

As discussed above, form VIII shows a unique resonance at 17.3 ppm and form XI exhibits a unique resonance at 20.2 ppm while the resonance at 23.9 ppm is shared by both forms. Figure 3 shows the ^{13}C CP/MAS NMR spectra of the expanded region of the binary mixtures as a function of form VIII content. (Spectra are only shown up to 15% form VIII due to space limitation.) The empirical detection limit of form VIII in a form XI dominated environment is about 2% (Figure 3); this is derived from the detectable appearance of the 17.3 ppm resonance at this concentration level (notice that at 1% level, the 17.3 ppm peak is not detectable), which is primarily determined by the signal-to-background-ratio (SBR).

Composition of the binary polymorph mixtures can be directly determined utilizing the peak intensities and Eq. 2. Since the T_{CH} values are similar and the $T_{1\rho H}$ values are not dramatically different between forms VIII and XI, the factor $F_{VIII/XI}$ is essentially unity. This represents the simplest situation since the mole ratio between forms VIII and XI in the mixture, M^0_{VIII}/M^0_{XI}, equals to their intensity ratio, I_{VIII}/I_{XI}.

The intensity measurements should, strictly speaking, use the integrated peak area rather than the peak height since different degrees of line broadening may be involved in resonances of each polymorph. The peak areas of 17.3 ppm (form VIII) and 20.2 ppm (form XI) of the CP/MAS NMR spectra of the mixtures (Figure 3) were measured. The mixture composition determined by ^{13}C CP/MAS NMR is defined as w_{VIII}^{NMR} (%) representing the mole fraction of form VIII in the mixture and obtained by the following equation:

$$w^{NMR}_{VIII} = \frac{\frac{M^0_{VIII}}{M^0_{XI}}}{1 + \frac{M^0_{VIII}}{M^0_{XI}}} \cdot 100\% \qquad (4)$$

where the subscripts, VIII or XI, refer to form VIII or XI, respectively. Note that there is no fitting coefficient in this expression. The compositions, w_{VIII}^{NMR}, are reported in Table 1 and plotted against the known mass fraction of the mixture, w_{VIII}^{mass}, in Figure 4. A linear correlation between w_{VIII}^{NMR} and w_{VIII}^{mass} was obtained over the wide range of the mixture composition examined (2–50%, w/w). Also note that the errors of absolute quantitation (the differences between w_{VIII}^{NMR} and w_{VIII}^{mass}) are usually within 1–2% (Table 1). A linear least square analysis yielded a slope of 0.972 ± 0.026, an intercept of 0.112%, and the coefficient of determination (R^2) of 0.999.

Estimation of the peak intensity by measurement of the peak height is also in wide use. Peak height is more readily measurable than the peak area (especially true when the peaks of two forms are not well resolved; vide infra). Since similar linewidths were observed for 17.3 ppm and 20.2 ppm resonances (best evidenced by an equal peak height in the mixture

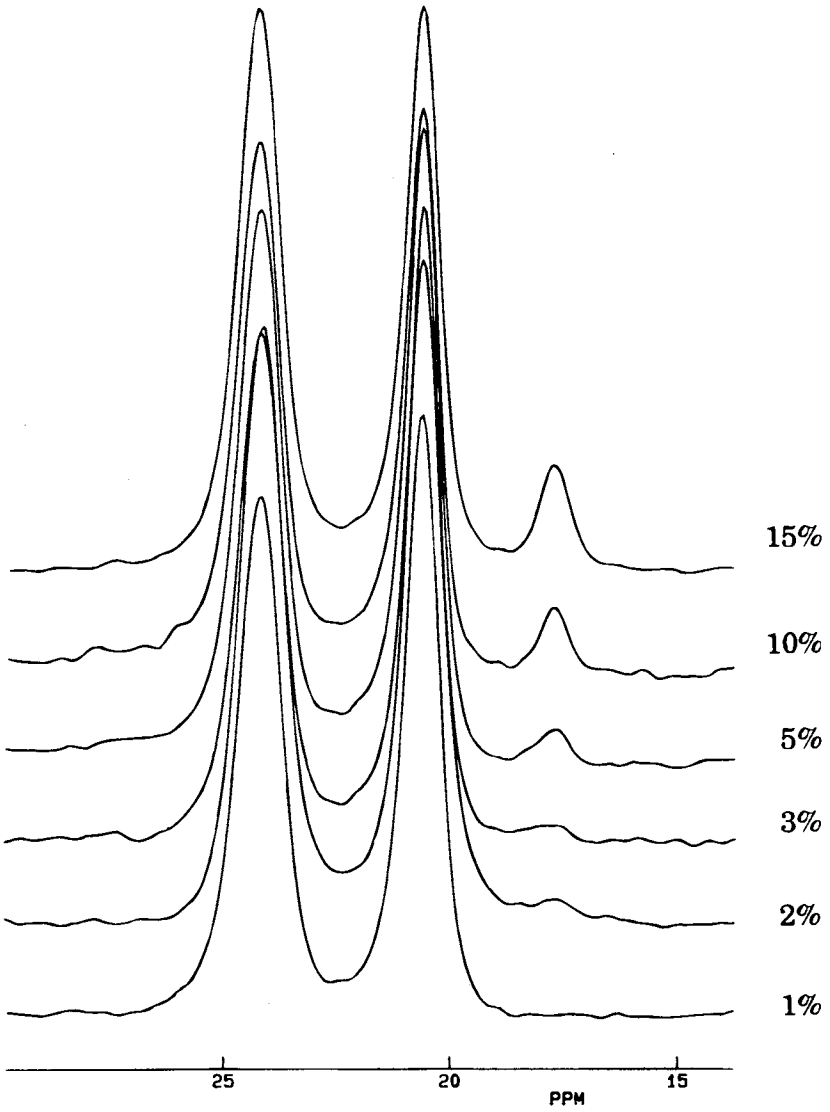

Fig. 3. Expanded region of ^{13}C CP/MAS NMR spectra of form VIII and XI mixtures with the mass fraction of form VIII indicated. Spectra were obtained using contact time = 2 ms; spinning rate = 3.5 kHz; and scan number = 1200.

containing 50% form VIII, not shown in Figure 3), their peak height ratio was deemed equivalent to the peak area ratio. The values of w_{VIII}^{NMR}, similarly derived using the peak height of the ^{13}C resonances and Eq. 4, are also reported in Table 1 and plotted against the mass fraction of the mixture, w_{VIII}^{mass}, in Figure 4 for comparison. Again, a good agreement with the mass fraction of the mixture was achieved and also with the quantitation using peak area. Linear least square analysis to this plot yielded a slope of 0.998 ± 0.035, an intercept of 0.239%, and the coefficient of determination (R^2) of 0.998 (Table 1).

Alternatively, the mixture composition can be determined by comparing the peak intensity of form VIII to the peak intensity representing both forms VIII and XI. This approach offers advantages especially when the diagnostic resonances due to different polymorphs substantially overlap. Again, the 17.3 ppm resonance intensity was used to represent the amount of form VIII. The 23.9 ppm resonance is shared by both forms and its intensity was assumed to represent the *total* amount of DLV-M. Both peak area and peak height were utilized for quantitation, and the results are reported in Table 1. Applications of linear least square fit to both plots yield a slope of 0.979 ± 0.026, an intercept of −0.092%, with R^2 = 0.999 for quantitation using the peak area; and a slope of 1.072 ± 0.080, an intercept of 1.074%, with R^2 = 0.994 for quantitation using the peak height.

Quantitation of Form XII and XI Mixtures

In contrast to quantitations of form VIII and XI mixtures, determination of the composition of form XII and XI mixtures presents a more challenging case. The dramatic difference of $T_{1\rho H}$s between forms XII ($T_{1\rho H}$ = 27.5 ms) and XI ($T_{1\rho H}$ = 447 ms) yields a value of 1.08 for $F_{XII/XI}$ according to Eq. 3. The value of $F_{XII/XI}$ implies that the peak intensity of the

Table 1. Compositions of Form VIII and XI Mixtures of DLV-M Determined Using ^{13}C Resonances (Either the Peak Area or the Peak Height as Indicated) and the Statistical Information of the Linear Least Square Analysis

Mixture	W_{VIII}^{mass} (%)	W_{VIII}^{NMR} (%)	W_{VIII}^{NMR} (%)	W_{VIII}^{NMR} (%)	W_{VIII}^{NMR} (%)
Reference		Figure 4	Figure 4	not shown	not shown
Method		A_{VIII}/A_{XI}[a]	H_{VIII}/H_{XI}[b]	$A_{VIII}/A_{VIII+XI}$[a]	$H_{VIII}/H_{VIII+XI}$[b]
	2.0	2.7	2.7	2.2	2.6
	3.0	2.8	2.8	3.0	3.3
	5.0	5.4	5.4	4.8	6.3
	10.0	9.4	10.2	9.1	11.8
	15.0	14.5	15.6	14.2	18.5
	19.9	20.2	20.3	19.9	24.8
	25.0	24.0	24.0	24.4	26.4
	50.0	48.7	50.5	48.9	54.0
intercept (%)		0.112	0.239	−0.092	1.074
slope		0.972	0.998	0.979	1.072
SD of slope		0.026	0.035	0.026	0.080
R^2		0.999	0.998	0.999	0.994
ESD (%)		0.444	0.601	0.389	1.371

[a] A: the ^{13}C resonance peak area.
[b] H: the ^{13}C resonance peak height.

methyl group of form XI is substantially greater than the peak intensity of the counterpart of form XII on an equal mole basis.

The CP/MAS NMR spectra of these mixtures are shown in Figure 5. The diagnostic peaks of form XII (19.1 ppm and 21.2/22.2 ppm) (*vide supra*) are close to the diagnostic peaks of form XI (20.2 ppm and 23.9 ppm), and they are not fully resolved in the spectra of the mixtures. In particular, the carbon resonances of form XII are not directly observable even at moderate concentrations in the mixtures (<20%) (Figure 5). Only at relatively high concentrations (>20% form XII), do the 19.1 and 21.2/22.2 ppm resonances of form XII appear as shoulders on the sides of the dominant 20.2 and 23.9 ppm peaks (form XI). Therefore, a different approach was developed to extract form XII peak intensities. A *difference* spectrum was obtained by subtracting the spectrum of pure form XI (Figure 1A) from each spectrum of the mixture (Figure 5). Difference spectra are shown in Figure 6 and exhibit characteristic features of pure form XII (being a criterion for adjustment of the subtraction) provided that form XI peaks are exactly cancelled out. Similar to form VIII and XI mixtures, the "visual" detection limit of form XII in the dominant form XI environment using ^{13}C CP/MAS NMR is about 3% (Figure 6) due to the SBR limit (S/N ≈ 2).

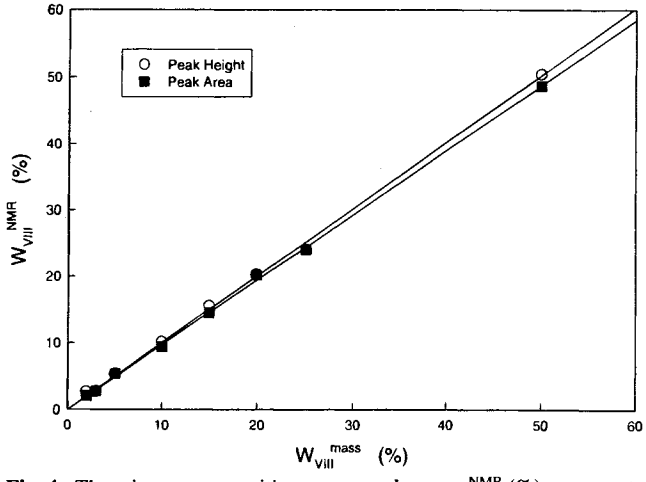

Fig. 4. The mixture composition, expressed as w_{VIII}^{NMR} (%), representing the mole fraction of form VIII in its mixtures with form XI, plotted against the mass fraction of form VIII, w_{VIII}^{mass}. The compositions are determined utilizing either the peak area (■) or the peak height (○).

Determination of the mixture composition is, therefore, obtained through measurements of the peak area of 19.1 ppm in the *difference* spectra (Figure 6), representing the amount of form XII, and measurements of the peak area of 20.2 ppm in the *original* spectra of the mixture (Figure 5), which inevitably includes the contribution of 19.1 ppm resonance and represents the total amount of DLV-M. The mixture composition determined by NMR is defined as w_{XII}^{NMR} (%), representing the mole fraction of form XII, and obtained by using a slightly different analytical procedure:

$$w_{XII}^{NMR} = \frac{M_{XII}^0}{M_{XII}^0 + M_{XI}^0} 100\% = \frac{F_{XII/XI} I_{XII}}{F_{XII/XI} I_{XII} + I_{XI}} 100\% \approx F_{XII/XI} \cdot \left(\frac{I_{XII}}{I_{XII+XI}}\right) 100\% \quad (5)$$

where the subscripts, XII and XI, are referred to forms XII and XI, respectively. Eq. 5 is an extension of Eq. 2, which correlates $M^0_{XII}/(M^0_{XII} + M^0_{XI})$ with the measurable peak intensity ratio, $I_{XII}/(I_{XII+XI})$. Notice that the term $F_{XII/XI}$ (=1.08) that appears in the denominator is treated as unity for simplification. In principle, this simplification may only introduce significant errors of the quantitation at high concentrations of form XII (>25%). The values of w_{II}^{NMR}, thus obtained, are reported in Table 2; the absolute quantitation error was usually within 2%. A linear least square analysis yields a slope of 0.955 ± 0.092,

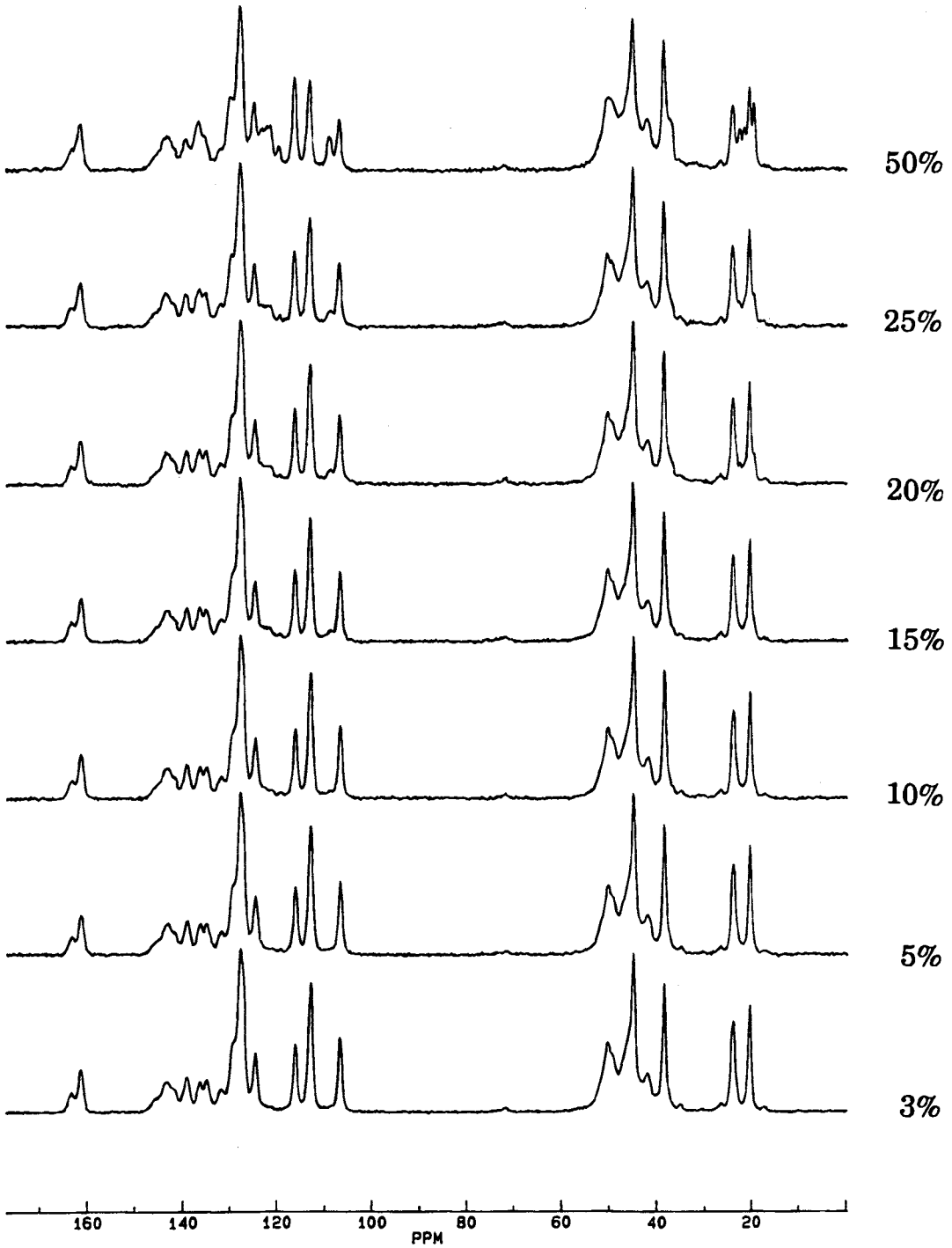

Fig. 5. ^{13}C CP/MAS NMR spectra of form XII and XI mixtures with the mass fraction of form XII indicated. Spectra were obtained using contact time = 2 ms; spinning rate = 4.5 kHz; and scan number = 640.

an intercept of 0.258%, and the coefficient of determination $R^2 = 0.993$.

The utilization of peak heights for quantitation was also examined. Again, the 19.1 ppm peak height observed in the difference spectra (Figure 6) represented the amount of form XII, whereas the 20.2 ppm peak height in the original spectra of the mixtures (Figure 5) represented the amount of form XI, rather than the total amount of DLV-M. This condition applied because the two resonances were reasonably resolved, and their peak heights did not significantly interfere with each other. This approach eliminated tedious peak area measurements with less operator dependent baseline determination and phase adjustment (*vide infra*). However, the 19.1 ppm resonance of form XII is slightly broader than the 20.2 ppm resonance of

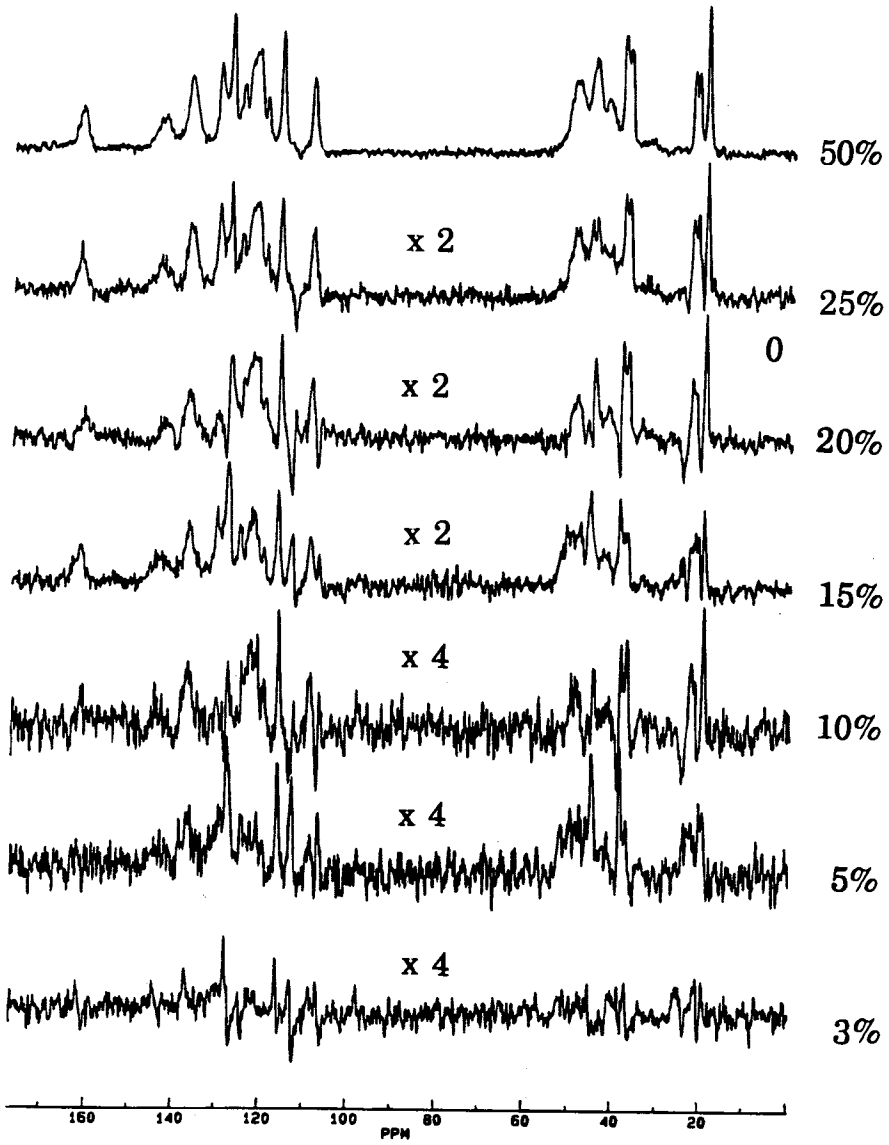

Fig. 6. Difference ^{13}C CP/MAS NMR spectra of form XII and XI mixtures with the mass fraction of form XII indicated. These spectra were obtained by subtracting the spectrum of form XI (Figure 1A) from the corresponding CP/MAS NMR spectra of the mixtures shown in Figure 5. Note that different scales are used.

form XI, primarily assumed to result from differences in crystal packing (14). Therefore, the peak height ratio was not equivalent to the peak area ratio. A proportionality constant, k, was empirically determined using Eq. 6 that correlated the peak height ratio with the peak area ratio for the pair of resonances of forms XII and XI:

$$\frac{A_{XII}}{A_{XI}} = k \cdot \left(\frac{H_{XII}}{H_{XI}}\right) \tag{6}$$

where A refers to the peak area and H the peak height. The constant k was essentially an indicator reflecting the relative broadness of the pair of resonances. The value of k (= 1.074) was best obtained from the measurements of both peak areas and peak heights observed in the difference spectra of form XI (not shown) and form XII (Figure 6), respectively, from the 49.7% mixture spectrum. Assuming k remains essentially unchanged in all these mixtures, values of w_{XII}^{NMR} were obtained using Eq. 2, 4, and 6, and are also reported in Table 2. Applying linear least square fit of w_{XII}^{NMR} vs. w_{XII}^{mass} gave a slope of 0.960 ± 0.067, an intercept of 0.331%, and a coefficient of determination R^2 of 0.996.

Alternatively, peak heights of the 22.2 ppm resonance (form XII) and the 23.9 ppm resonance (form XI) can also be used for quantitation. These results are also reported in Table 2 for comparison. This approach gave similar result with comparable precision (linear least square fit: slope = 0.963 ± 0.071, intercept = 0.742%, and R^2 = 0.996).

Quantitation Errors

Errors in quantitative analysis using ^{13}C CP/MAS NMR can arise from several sources excluding the experimental errors: (i) poor signal-to-noise (s/n) ratios, especially for the low concentrations of minor polymorphic form in the mixtures;

Table 2. Compositions of Form XII and XI Mixtures of DLV-M Determined Using ^{13}C Resonances (Either the Peak Area or the Peak Height as Indicated) and the Statistical Information of the Linear Least Square Analysis

Mixture	W_{XII}^{mass} (%)	W_{XII}^{NMR} (%)	W_{XII}^{NMR} (%)	W_{XII}^{NMR} (%)
Method		A_{XII}/A_{XII+XI}[a]	H_{XII}/H_{XI}[b]	H_{XII}/H_{XI}[b]
	1.9	—	—	—
	3.0	3.6	3.0	3.3
	5.0	5.8	4.9	5.7
	9.9	9.7	9.9	9.6
	14.9	11.9	13.3	15.5
	19.9	20.7	21.0	19.0
	24.9	23.7	25.0	26.7
	49.7	48.0	47.5	48.0
intercept(%)		0.258	0.331	0.742
slope		0.955	0.960	0.963
SD of slope		0.092	0.067	0.071
R^2		0.993	0.996	0.996
ESD (%)		1.398	1.021	1.082

[a] A: the ^{13}C resonance peak area.
[b] H: the ^{13}C resonance peak height.

(ii) improper phase adjustment; and (iii) improper baseline correction.

Poor s/n may be partially compensated by extensive signal averaging with a relatively large number of accumulated scans (>1000) (20). Although the s/n of the ^{13}C CP/MAS NMR spectrum may be slightly improved by acquiring significantly more scans, the visual detection limit (ca. 2–3%) of the minor form in the two cases seems not affected.

Although peak area, in principle, best represents the intensity and, therefore, the analytical quantity, peak area is often greatly affected by the phase adjustment and baseline correction, which are usually subjective and operator dependent. Phase adjustment is a critical element, especially for computing the *difference* spectra. A statistical average of several measurements ($n \geq 3$) of the same peak area, which involve different degree of plot expansion and base line correction, usually minimizes subjectivity and improves quantitative precision. However, experience suggests that measurement of the peak height appears to be less sensitive to the phase adjustment than the peak area. Furthermore, peak height measurements are more straightforward and probably less operator-dependent than peak area measurements. Conversely, peak height based quantitation may yield results with somewhat lower precision. Errors in measurements of the peak area or peak height are the key source of quantitation error. Partially because (ii) and (iii) are more difficult to control over a wide region of the spectrum, reasonable quantitative results are best obtained by selecting well-resolved resonances of the same type within a limited spectral region and using the peak height if appropriate.

Statistical results of the linear least squares analyses for all quantitation results discussed above are summarized in Tables 1–2. The estimated standard deviation of the linear least squares analysis, ESD, is defined by Eq. 7:

$$ESD = \left[\frac{\Sigma\,(w^{NMR} - w^{est})^2}{(n-2)}\right]^{1/2} \qquad (7)$$

The sum extends over n observations; w^{NMR} is the composition determined by NMR; and w^{est} is the estimated fraction by the linear least squares fit for each mixture. The ESD term provides a gross overall estimate of the precision regarding the quantitation using ^{13}C CP/MAS NMR. In addition, ESD term appears to have a larger capacity to differentiate the quality of the fit of different analytical approaches than other statistical terms.

Comparing the ESDs reported in Table 1 for the quantitation of forms VIII and XI mixtures, similar ESDs of w_{VIII}^{NMR} (0.44 to 0.60%) were achieved using either the peak area ratio or the peak height ratio for the 17.3/20.2 ppm pair of resonances, representing I_{VIII}/I_{XI}. A larger ESD (1.37%) was obtained when the peak height ratio for the pair of 17.3/23.9 ppm, representing $H_{VIII}/(H_{VIII+XI})$, was used for quantitation; a smaller ESD (0.38%) was obtained using the peak area of the same peaks. These results suggest that better precisions can be achieved using peak area measurements. However, for quantitations of forms XII and XI mixtures, a slightly larger ESD (1.40%) is observed using the peak area compared to the ESDs (1.02–1.08%) using the peak height (Table 2). The difference in this case was presumably attributed to the overlapping of resonances of the two forms, causing larger errors in peak area measurements due to spectral subtraction inefficiency. In such cases, measurements of peak height appear to provide better precision than measurements of peak area due to less subjectivity. In general, the ESDs of the quantitation of forms XII and XI mixtures (Table 2) are two to three fold larger compared to the ESDs of the quantitation of form VIII and XI mixtures (Table 1) using the same approach. This is most likely attributed to the two factors: (i) the interference of the intensity measurement of analytical peaks due to substantial overlapping, and (ii) the dramatically different relaxation times between the two components.

Empirical detection limit using ^{13}C CP/MAS NMR in these two cases was estimated to be 2–3%. Assuming that the detection is limited by background noise, the detection limit, DL (w/w, %), of form VII, or form XII, in a form XI dominated environment can be calculated by the SBR/RSDB(relative standard derivation of the background) analysis (21):

$$D_L = k \cdot 0.01 \cdot RSDB \cdot \frac{C_0}{SBR} \qquad (8)$$

Where RSDB is expressed as a percentage and SBR is associated with concentration C_0 yielding a net analyte signal. In this work, SBR $\approx$ 2 was used when $C_0 \approx 2\%$ (form VIII), or 3% (form XII), and RSDB $\approx$ 30%; k = 3 was used as generally recommended (21). Thus, the calculated detection limit was 1% for form VIII, or 1.5% for form XII, which was in reasonable agreement with the "visual" detection limits.

CONCLUSIONS

This study demonstrates that ^{13}C CP/MAS NMR has the ability to differentiate pharmaceutical polymorphs and pseudopolymorphs, and to quantitate reliably the relative amounts of each form in their mixtures in a rapid and non-destructive manner. The greatest advantage of this technique lies in the unambiguous identification of the minor polymorphic or pseudopolymorphic form in the dominant environment of the other form with empirical detection limits about 2–3%. Based upon the cross-polarization and relaxation kinetics considerations, appropriate analytical procedures were developed for ^{13}C CP/MAS NMR. Quantitative results using ^{13}C intensities indicate a linear correlation with the

mass fractions of these mixtures over a wide concentration range (2–50% of the minor form). In this application, no calibration efforts are needed; however, a reliable measurement of NMR relaxation times ($T_{1\rho H}$, T_{1H}) and heteronuclear CP rate constant (T_{CH}) is a critical requirement of the method. The analytical procedure for ^{13}C CP/MAS NMR developed in this study may be generally applicable for quantitative analysis of pharmaceutical solid mixtures (i.e., bulk drugs, dosage forms), provided that distinctly resolved NMR resonances of each form are observed and their relaxation behaviors are well characterized.

ACKNOWLEDGMENTS

The author would like to thank Paul Fagerness, Mike Bergren, Gary Martin, and John Stodola for helpful discussions and comments on the manuscript; Mike Bergren and Lisa Madden for preparing all DLV-M mixtures; and Ken Visscher for technical support. The author also wishes to thank Ken Manning and John Landis for supporting the solid-state NMR program.

REFERENCES

1. I. W. Althaus, J. J. Chou, A. J. Gonzales, M. R. Deibel, K-C. Chou, F. J. Kezdy, D. L. Romero, R. C. Thomas, P. A. Aristoff, W. G. Tarpley, and F. Reusser. Kinetic studies with the non-nucleoside human immunodeficiency virus type-1 reverse transcriptase inhibitor U-90152E. *Biochemical Pharmacology.* **47**:2017–2028 (1994).
2. T. J. Dueweke, S. M. Poppe, D. L. Romero, S. M. Swaney, A. G. So, K. M. Downey, I. W. Althaus, F. Resser, M. Busso, L. Resnick, D. L. Mayers, J. Lane, P. A. Aristoff, R. C. Thomas, and W. G. Tarpley. U-90152, a potent inhibitor of human immunodeficiency virus type 1 replication. *Antimicrobial Agents and Chemotherapy.* **37**:1127–1131 (1993).
3. M. S. Bergren, R. S. Chao, P. A. Meulman, R. W. Sarver, M. A. Lyster, J. L. Havens, and M. Hawley. Solid phase diversity of delavirdine mesylate. Manuscript submitted to *J. Pharm. Sci.*
4. S. R. Byrn, R. Pfeiffer, M. Ganey, C. Hoiberg, and C. Poochikian. Pharmaceutical solids: A strategic approach to regulatory considerations. *Pharm. Res.* **12**:945–954 (1995).
5. D. E. Bugay. Solid-state nuclear magnetic resonance spectroscopy: Theory and pharmaceutical applications. *Pharm. Res.* **10**:317–327 (1993).
6. H. Y. Aboul-Enein. Applications of solid-state nuclear magnetic resonance spectroscopy to pharmaceutical research. *Spectroscopy.* **5**:32–40 (1990).
7. H. G. Brittain, S. J. Bogdanowich, D. E. Bugay, J. DeVincentis, G. Lewen, and A. W. Newman. Physical characterizations of pharmaceutical solids. *Pharm. Res.* **8**:963–973 (1991).
8. J. S. Bernstein. Nuclear magnetic resonance in pharmaceutical technology. in J. Swarbrick and J. C. Boylan (eds.), *Encyclopedia of Pharmaceutical Technology.* Marcel Dekker, Inc. New York, 1994. Vol. 10, pg 335–353.
9. P. J. Saindon, N. S. Cauchon, P. A. Sutton, C-j. Chang, G. E. Peck, and S. R. Byrn. Solid-state nuclear magnetic resonance (NMR) spectra of pharmaceutical dosage forms. *Pharm. Res.* **10**:197–203 (1993).
10. R. K. Harris. *Nuclear magnetic resonance spectroscopy.* Pitman Publishing, Inc. , Marshfield, MA, 1983. pg111.
11. R. Suryanarayanan, and T. S. Wiedmann. Quantitation of the relative amounts of anhydrous carbamazepine ($C_{15}H_{12}N_2O$) and carbamazepine dihydrate ($C_{15}H_{12}N_2O{\cdot}2H_2O$) in a mixture by solid-state nuclear magnetic resonance (NMR). *Pharm. Res.* **7**:184–187 (1990).
12. J. S. Fyre and G. E. Maciel. Setting the magic angle using a quadrupolar nuclide. *J. Mag. Res.* **48**:125–131 (1982).
13. L. W. Jelinski, and M. T. Melchior. High–resolution NMR of solids. in C. Dybowski and R. L. Lichter (eds.), *NMR Spectroscopy Techniques.* Marcel Dekker, Inc., New York, 1985.
14. P. Gao. Manuscript in preparation for *Pharm Res.*
15. L. B. Alemany, D. M. Grant, R. J. Pugmire, T. D. Alger, and K. W. Zilm. Cross polarization and magic angle spinning NMR spectra of model organic compounds 1. Highly protonated molecules. *J. Am. Chem. Soc.* **105**:2133–2147 (1985).
16. M. Mehring. *Principles of high resolution NMR in solids.* 2 ed. Springer-Verlag, New York, 1983. Chapter 4.
17. R. K. Harris. Quantitative aspects of high-resolution solid-state nuclear magnetic resonance spectroscopy. *Analyst.* **110**:649–655 (1985).
18. A. Jurkiewicz, and G. E. Maciel. ^{13}C NMR spin-lattice relaxation properties and quantitative analytical methodology of ^{13}C NMR spectroscopy for coals. *Anal. Chem.* **67**:2188–2194 (1995).
19. D. G. Rethwisch, M. A. Jacintha, and C. R. Dybowski. Quantitation of ^{13}C in solids using CPMAS-DD-NMR spectroscopy. *Anal. Chim. Acta.* **283**:1033–1043 (1993).
20. An alternative approach to improve S/N is to use a large rotor assuming enough sample aviliable.
21. P. W. J. M. Boumans. Detection limits and spectral interferences in atomic emission spectroscopy. *Anal. Chem.* **66**:459A–467A (1994).